

UCSF

UC San Francisco Previously Published Works

Title

Magnetic Catheter Manipulation in the Interventional MR Imaging Environment

Permalink

<https://escholarship.org/uc/item/04v5j8qh>

Journal

Journal of Vascular and Interventional Radiology, 24(6)

ISSN

1051-0443

Authors

Wilson, Mark W
Martin, Alastair B
Lillaney, Prasheel
[et al.](#)

Publication Date

2013-06-01

DOI

10.1016/j.jvir.2013.01.487

Peer reviewed

Published in final edited form as:

J Vasc Interv Radiol. 2013 June ; 24(6): 885–891. doi:10.1016/j.jvir.2013.01.487.

Magnetic Catheter Manipulation in the Interventional MRI Environment

Mark W. Wilson, MD¹, Alastair B. Martin, PhD¹, Prasheel Lillaney, PhD¹, Aaron D. Losey, MS¹, Erin J. Yee, BS¹, Anthony Bernhardt, PhD², Vincent Malba, PhD², Lee Evans, BS², Ryan Sincic, MS, NP¹, Maythem Saeed, PhD, DVM¹, Ronald L. Arenson, MD¹, and Steven W. Hetts, MD¹

¹Department of Radiology and Biomedical Imaging, University of California San Francisco, San Francisco, California

²Lawrence Livermore National Laboratory, Livermore, California

Abstract

Purpose—To evaluate deflection capability of a prototype endovascular catheter, which is remotely magnetically steerable, for use in the interventional MRI environment.

Materials and Methods—Copper coils were mounted on the tips of commercially available 2.3 – 3.0 Fr microcatheters. The coils were fabricated in a novel manner by plasma vapor deposition of a copper layer followed by laser lithography of the layer into coils. Orthogonal helical (solenoid) and saddle-shaped (Helmholtz) coils were mounted on a single catheter tip. Microcatheters were tested in water bath phantoms in a 1.5T clinical MRI scanner, with variable simultaneous currents applied to the coils. Catheter tip deflection was imaged in the axial plane utilizing a “real-time” steady-state free precession (SSFP) MRI sequence. Degree of deflection and catheter tip orientation were measured for each current application.

Results—The catheter tip was clearly visible in the longitudinal and axial planes. Magnetic field artifacts were visible when the orthogonal coils at the catheter tip were energized. Variable amounts of current applied to a single coil demonstrated consistent catheter deflection in all water bath experiments. Changing current polarity reversed the observed direction of deflection, whereas current applied to two different coils resulted in deflection represented by the composite vector of individual coil activations. Microcatheter navigation through the vascular phantom was successful through control of applied current to one or more coils.

© 2013 The Society of Interventional Radiology. Published by Elsevier Inc. All rights reserved.

Corresponding Author: Steven W. Hetts, MD, 185 Berry Street, Suite 350, San Francisco, CA 94107, Department of Radiology and Biomedical Imaging, University of California, San Francisco, Phone: (415) 206-6607, Fax: (415) 206-4004, Steven.Hetts@ucsf.edu.

Financial Disclosures:

NIH National Heart Lung Blood Institute (NHLBI) Award (M. Wilson): 1R01HL076486 American Society of Neuroradiology Research and Education Foundation Scholar Award (S. Hetts)

NIH National Institute of Biomedical Imaging and Bioengineering (NIBIB) Award (S. Hetts): 1R01EB012031

This material was presented by Dr. Mark W. Wilson at the 37th Annual Scientific Meeting of the Society of Interventional Radiology in March 2012.

Conflicts of Interest:

Dr. Steven W. Hetts has received grant support from Stryker Corporation, is a paid consultant for Silk Road Medical, and is a member of the scientific advisory board of Medina.

Publisher's Disclaimer: This is a PDF file of an unedited manuscript that has been accepted for publication. As a service to our customers we are providing this early version of the manuscript. The manuscript will undergo copyediting, typesetting, and review of the resulting proof before it is published in its final citable form. Please note that during the production process errors may be discovered which could affect the content, and all legal disclaimers that apply to the journal pertain.

Conclusion—Controlled catheter deflection is possible with laser lithographed multi-axis coil tipped catheters in the MRI environment.

Introduction

Image-guided endovascular procedures are increasingly common. Although most of these procedures are performed under x-ray fluoroscopic guidance, x-ray imaging does not have the ability to depict soft tissue structure and physiology as well as MRI. If endovascular procedures can be performed partially or completely under MRI guidance, then real time monitoring of tissue physiology—including temperature, perfusion, and diffusion (the gold standard for cerebral infarction, for example)—then interventionalists could have better ability to assess the success of their procedures.

Maneuvering a catheter during procedures performed partially or completely under MRI guidance is presently more challenging than under x-ray fluoroscopy, as most standard catheters and guidewires have ferromagnetic components that make them incompatible with MRI. We propose a magnetic guidance system comprised of a microcatheter with copper coils implanted on the catheter tip, which can be deflected in the strong magnetic field of an MRI scanner when a current is applied to the catheter tip. The induced magnetic moment will seek to align with the B_0 field of the scanner, thus deflecting the catheter tip and allowing controlled advancement of the catheter under real time MR imaging (9). Using a novel method of laser lithography, copper coils can be fabricated on cylinders and attached to the tips of angiographic catheters. Both solenoid and Helmholtz saddle-shaped coils can be patterned using the same lithographic technique. This allows deflection of the catheter tip in multiple directions by the generation of magnetic moment vectors relative to the B_0 field of the MRI scanner. Our microcoil tipped catheter system can be used in any clinical MRI scanner for magnetic guidance and imaging. The purpose of these experiments was to test the hypothesis that a microcatheter with orthogonal coils mounted on its tip can be controllably and actively deflected in several directions in the MRI scanner when currents are applied to the coils and to demonstrate that the catheter movement can be visualized on dynamic MR images.

Materials and Methods

Microcatheter Selection

Commercially available 150 cm catheters (Tracker 18-103101 and 18-103102, and Renegade-18-253, Boston Scientific, Natick, MA, USA) were used as substrates. The microcatheters ranged in size from 2.3 F to 3.0 F at the catheter tip, which are standard sizes used for neurological and body interventional procedures.

Details of Coil Fabrication

The coils, both helical (solenoid) and saddle (Helmholtz), were fabricated with a lithographic technique called Laser Lathe, which allows non-planar surfaces such as cylinders to be patterned with feature sizes as small as 5 μm . The cylinder material of choice for this project was commercially available Kapton polyimide film (DuPont, Wilmington, DE, USA) because it is both chemically and thermally inert to the processing conditions required. In order to improve the adhesion of deposited films to the polyimide, the cylinders were exposed to an oxygen plasma to roughen the surface and remove impurities prior to sputter deposition. A conductive coating (a “seed layer”) consisting of a copper layer (~200 nm) over a titanium layer (~50 nm) was deposited on the polyimide surface with an MRC 8671 sputtering system, fitted with a rotary fixture for uniform deposition on a cylinder. The purpose of the Titanium/Copper seed layer was to create a conductive layer onto which a positive electrodeposited photoresist (Shipley’s PEPR-2400) could be electroplated. This

PEPR coating provided a uniform photoactive layer on the surface that could be patterned with a laser.

Figure 1 shows a schematic of the Laser Lathe apparatus. It consists of three high-precision air-bearing translation stages (x, y, and z), and one high-precision rotary stage. The axis of the rotary stage is parallel to the translation of the x stage. A 405-nm, 50 mW diode laser is used to expose the PEPR photoresist. The z-stage is used to focus the beam by moving a microscope objective through which the beam is passing. With precision motion control of the stages provided by a PMAC card (Delta Tau Data Systems, Inc., Chatsworth, CA, USA), any coil design can be patterned on the surface of the cylinder. Figure 2 shows a helical coil, saddle coil, and two saddle coils patterned side by side at 90 degrees with respect to each other in panels A through C respectively.

Coil-to-Catheter Assembly

One-, two-, and three-axis coils were fabricated with the Laser Lathe process. The coils were manufactured on individual tubes of different diameters, and inserted one coil inside another (Figures 3 and 4).

Devices were then assembled by running the required number of 0.005'' wires (2 for 1-axis, 4 for 2-axis, and 6 for 3-axis) through the entire length of the microcatheter lumen. Then, 0.002'' wire was soldered to the 0.005'' wire at the catheter tip, and was fed through holes that had been drilled in the polyimide tube near the coil connection pads. The 0.002'' wires were then soldered to the coil connection pads. The polyimide tube was then glued to the tip of the microcatheter and secured with heat shrink tubing (Raychem, North Spring, TX, USA). The final outer diameter of the catheter tip with coils and shrink wrap applied was approximately 2 mm (6 Fr). The 0.005'' copper wires at the microcatheter hub were connected to a 5-pin or 8-pin electrical connector (a male telephone or Ethernet jack). The jack was plugged into a female connector on an electrical switch box (used to change the electrical polarity of the DC currents), which was connected to up to 3 DC power supplies.

MRI phantom studies

The MRI phantom studies were performed using a 1.5 Tesla, short-bore Achieva MR imager (Philips Medical Systems, Best, The Netherlands). Passive MR imaging was performed at a frame rate 2 to 5 images per second. The actual imaging sequence empirically judged to be most suitable was a SSFP dynamic sequence. This is a fast gradient echo sequence with the following parameters: TR = 5.5 ms, TE = 1.6 ms, flip angle = 30°, 128 × 128 matrix, 5–6 mm slice thickness. An 8-channel head coil was used to improve the signal-to-noise ratio. Images from this sequence clearly showed the non-energized stationary catheter, all in-plane catheter movements, and field inhomogeneity artifact at the tip of the energized catheter. The SSFP sequence also imparts high signal intensity to fluid-filled structures flowing and stationary, thereby providing a suitable background contrast for the catheters.

All catheters were tested in the same open water bath, MR-compatible phantom. By simultaneously energizing combinations of one or both coils with currents of variable strength and polarity, the catheter tip would be deflected in several directions. The deflection angle and orientation of the catheter tip was measured on the MR images. The deflection angle in the longitudinal plane was measured relative to a line drawn down the catheter shaft. The position of the catheter tip in the axial plane was determined relative to the horizontal x-axis, which was designated as 0 degrees.

Finally, a MRI-compatible bifurcated phantom was fabricated from clear acrylic tubing (Interstate Plastics, Sacramento, CA, USA). The larger "vessel" component of the phantom

measured 2 cm in diameter, while the branch “vessels” measured 1 cm in diameter. This phantom was used to test the catheters in a simulated clinical setting.

Results

Microcatheter Tip Visualization

In all experiments, the tip of the microcatheter was clearly visible as a dark MR artifact when current was applied during imaging. Artifact shape and size varied and were determined by the number of coils activated at a given time and the tip’s orientation relative to the magnetic field of the scanner. Small amounts of current not sufficient to cause deflection permitted quick location of the catheter tip.

Microcatheter Water Bath Experiments

Experiments performed in water bath phantoms demonstrated predictable, controllable tip deflection under MRI at various current levels. Deflection experiments where a single coil was energized with positive current were performed by two investigators blinded to each others’ measurements. These experiments were performed with either 2cm or 5cm unrestrained catheter lengths extending into the water bath. The data is summarized in the Tables 1 and 2.

Activation of one coil with a given amount of current consistently led to a specific degree of observed deflection as shown above and in Figure 6. Activation of the same coil with the same amount of current but reversed in polarity resulted in the same degree of observed deflection within the same plane but in the opposite direction (Figure 6). Combinations of current sent to two coils, designated Coil A and Coil B, resulted in longitudinal deflection that is the vector sum of the two individual deflection angles. For example, current “A+” produced a 17° deflection and “B-” produced an 18° deflection whereas a combination of current “A+B-” delivered simultaneously to coils resulted in the expected tip deflection of 23°. The orientations of the deflected catheter tips in the axial plane were clearly visible on the dynamic MR images (Figure 7). By applying various amplitudes, polarities, and combinations of current to one or more coils, the catheter tip can be deflected in almost any desired direction in the axial plane, as summarized in Figure 8.

Bifurcation Phantom Experiments

Experiments in the Y shaped vascular phantom, designed to simulate the human aorta, further supported the controllable deflection capabilities of the catheter tip under MRI. The tip of the microcatheter was easily visible during imaging and was used as a tracking tool throughout the experiment. Activation of current in one or more of the coils along with manual advancement of catheter allowed successful navigation in to the left branch of phantom (Online Figure 9A). The catheter was manually retracted back to the vessel bifurcation. Successful remote-controlled deflection was then performed with opposite coil current polarity to guide the catheter into the opposite branch of the phantom (Online Figure 9B).

Discussion

Performing endovascular interventions under MRI guidance is challenging, as most standard clinical guidewires and catheters for use under x-ray fluoroscopy have ferromagnetic components that preclude their use in MRI. In order to take advantage of MRI as a real time interventional guidance modality—and thus open up its possibilities of intraprocedural tissue physiological monitoring with diffusion and perfusion MR techniques—catheters that can navigate the blood vessels under MRI guidance and safely remain there during MR

imaging need to be developed. This investigation focused on remote control catheter navigation, a way of overcoming the challenge of maneuvering catheters under MRI guidance when standard guidewires and catheters are not safe to use.

Others have recognized the limitations of current catheter navigation techniques and attempted to develop systems that assist with catheter manipulation by allowing the catheter or guidewire tip to deflect. Several past studies describe deflection of a modified guidewire with magnet containing tip under a magnetic guidance system consisting of two magnets positioned around the operating table. This system, however, is limited due to the required use of the permanent, external magnetic system and separate, modified C-arm angiography system for imaging (4–6). Also, the use of large, movable, external magnets makes this system inherently incompatible with real time MR imaging. Another study demonstrated a catheter system that could achieve deflection under magnetic resonance imaging by placing one to three soft ferromagnetic spheres encased at the distal tip of a commercially available microcatheter (7, 8). However, dipole-dipole interactions between spheres can lead to undesirable jumping displacement, preventing precise control of the catheter tip. Additionally, a lack of increase in tip deflection after the addition of two beads to the tip and the bead diameter is a limiting factor of the system design (7, 8).

Laser lithography permits patterning of a microcatheter tip with up to three orthogonal coils (single z-axis solenoid and x- and -y axis Helmholtz coils). Using this novel technique, we demonstrated that activation of current through one or more of these coils produced controllable catheter tip deflection under MR imaging. By keeping the number of solenoid coil turns, catheter stiffness, and external magnetic field strength constant, we were able to produce predicted angles of deflection from application of various current levels as determined by the equation derived by Settecase et al (1). Additionally, increases in current resulted in larger angles of deflection without uncontrolled tip displacement as has been reported in the magnetic guidance system based on paramagnetic sphere-tipped catheters (7, 8). These findings support the notion that controlled steering of the distal catheter tip in almost any direction in three-dimensional space is possible. The exception to this is directly along the B_0 z-axis of the MRI scanner if the catheter is perfectly aligned with it at baseline.

Further investigation is needed to determine if integrating magnetic catheter deflection with navigation through difficult vasculature is more efficient than current endovascular techniques either under x-ray fluoroscopic guidance, under MRI guidance, or under combined guidance in multimodality interventional imaging suites.

When current is applied to it, the catheter tip is clearly observed as an MR artifact during imaging. The number of activated coils and the amount of current applied dictates the characteristic shape and size of the artifact. In the sphere-tipped catheter system, an artifact is continuously present because of the ferromagnetic material comprising the spheres (7, 8). Without applied current in our system, an MR artifact is absent. However, a small 'visualization' current may be applied to actively locate the position of catheter tip (10). The presence of an MR artifact can therefore be used as a convenient visualization and tracking tool of the distal tip of the microcatheter during an endovascular procedure.

Two limitations in our experiments should be noted. Although the visualization of the catheter tip was confirmed during MRI in all experiments, no quantification of the MR artifact was conducted. Furthermore, catheter deflection angles were measured and recorded in single planes, as opposed to simultaneously in multiple planes. Future studies will incorporate the use of MR-compatible cameras positioned in two different dimensions to confirm the precise three-dimensional orientation of the catheter tip.

The catheter tip deflection and visualization capabilities displayed in these experiments set a foundation for this magnetic guidance system. These studies are early-stage investigations in simple vascular phantoms. We intend to conduct additional experiments in complex 3-D vascular models and *in vivo*. In conjunction with safety studies addressing catheter heating (9, 11), these advances will bring us further in the development of a magnetically assisted remote controlled catheter system for image-guided endovascular procedures that can be used in any MRI scanner or hybrid X ray/MRI suite.

Acknowledgments

We would like to thank Joey English, MD, PhD, Pallav Kolli, MD, Fabio Settecase, MD, MSc, Timothy P. Roberts, PhD, and Bill Hassenzahl.

References

1. Settecase F, Sussman MS, Wilson MW, et al. Magnetically-assisted remote control (MARC) steering of endovascular catheters for interventional MRI: a model for deflection and design implications. *Med Phys*. 2007; 34:3135–142. [PubMed: 17879774]
2. McDougall CG, Halbach VV, Dowd CF, Higashida RT, Larsen DW, Hieshima GB. Causes and management of aneurysmal hemorrhage occurring during embolization with Guglielmi detachable coils. *J Neurosurg*. 1998; 89:87–92. [PubMed: 9647177]
3. Fu Y, Liu H, Huang W, Wang S, Liang Z. Steerable catheters in minimally invasive vascular surgery. *The International Journal of Medical Robotics + Computer Assisted Surgery: MRCAS*. 2009; 5:381–391. [PubMed: 19795440]
4. Schiemann M, Killmann R, Kleen M, Abolmaali N, Finney J, Vogl TJ. Vascular guide wire navigation with a magnetic guidance system: experimental results in a phantom. *Radiol*. 2004; 232:475–481.
5. Krings T, Finney J, Niggemann P, et al. Magnetic versus manual guidewire manipulation in neuroradiology: in vitro results. *Neuroradiology*. 2006; 48:394–401. [PubMed: 16622696]
6. Ramcharitar S, Patterson MS, van Geuns RJ, van Meighem C, Serruys PW. Technology Insight: magnetic navigation in coronary interventions. *Nat Clin Pract Cardiovasc Med*. 2008; 5:148–156. [PubMed: 18250634]
7. Gosselin FP, Lalande V, Martel S. Characterization of the deflections of a catheter steered using a magnetic resonance imaging system. *Med Phys*. 2011; 38:4994–5002. [PubMed: 21978043]
8. Lalande V, Gosselin FP, Martel S. Catheter steering using a Magnetic Resonance Imaging system. Conference proceedings: Annual International Conference of the IEEE Engineering in Medicine and Biology Society IEEE Engineering in Medicine and Biology Society Conference. 2010; 2010:1874–1877. [PubMed: 21096567]
9. Bernhardt A, Wilson MW, Settecase F, et al. Steerable catheter microcoils for interventional MRI reducing resistive heating. *Acad Radiol*. 2011; 18:270–276. [PubMed: 21075017]
10. Roberts TP, Hassenzahl WV, Hetts SW, Arenson RL. Remote control of catheter tip deflection: an opportunity for interventional MRI. *Magn Reson Med*. 2002; 48:1091–1095. [PubMed: 12465124]
11. Settecase F, Hetts SW, Martin AJ, et al. RF Heating of MRI-Assisted Catheter Steering Coils for Interventional MRI. *Acad Radiol*. 2011; 18:277–285. [PubMed: 21075019]

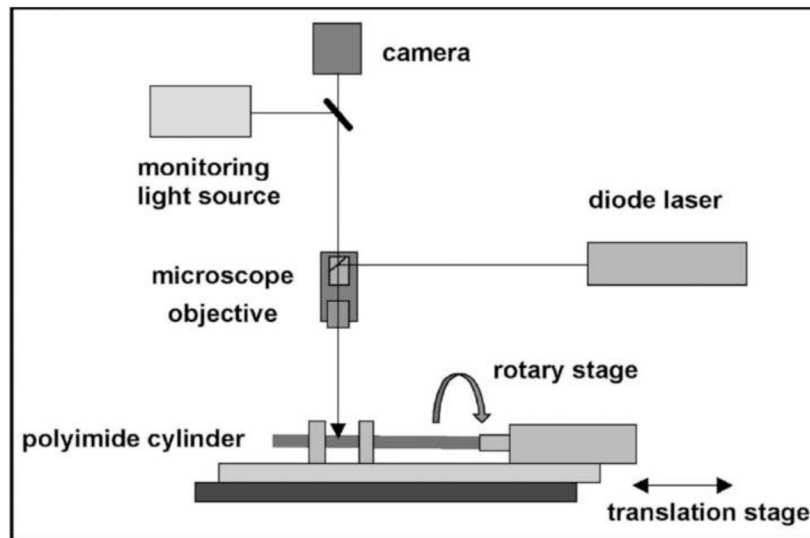


Figure 1. Schematic diagram of the Laser Lathe apparatus. The translational stage moves the polyimide cylindrical tip as it is rotated to allow etching of the helical (solenoid) coil on the cylinder. This cylinder will subsequently be mounted on the end of the microcatheter.

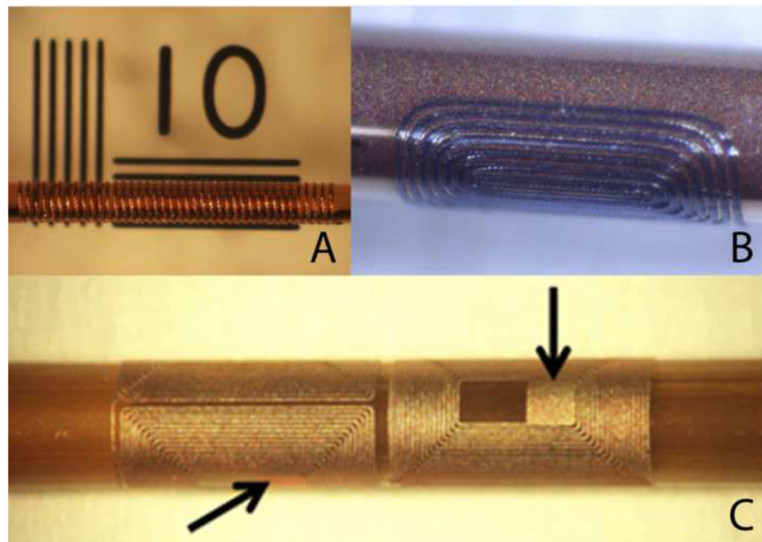


Figure 2.

A) A 50 turn helical coil patterned on a 1.37 mm OD polyimide cylinder. The copper wires are 50- μm wide, 15- μm thick, and have a 100- μm pitch. The resistance of the coil is 6-ohms. B) A 40-turn saddle (Helmholtz) coil (20 turns on opposite sides) patterned on a 1.7 mm OD polyimide cylinder. The copper lines are 20- μm wide, 15- μm thick, and have a 40- μm pitch. C) Two 30-turn saddle coils patterned side by side on a 1.37 mm OD polyimide cylinder. The copper lines are 20- μm wide, 15- μm thick, and have a 40- μm pitch. The coils are orthogonal with respect to each other. The solder attachment pads (arrows) are 500- μm wide and 500- μm long.

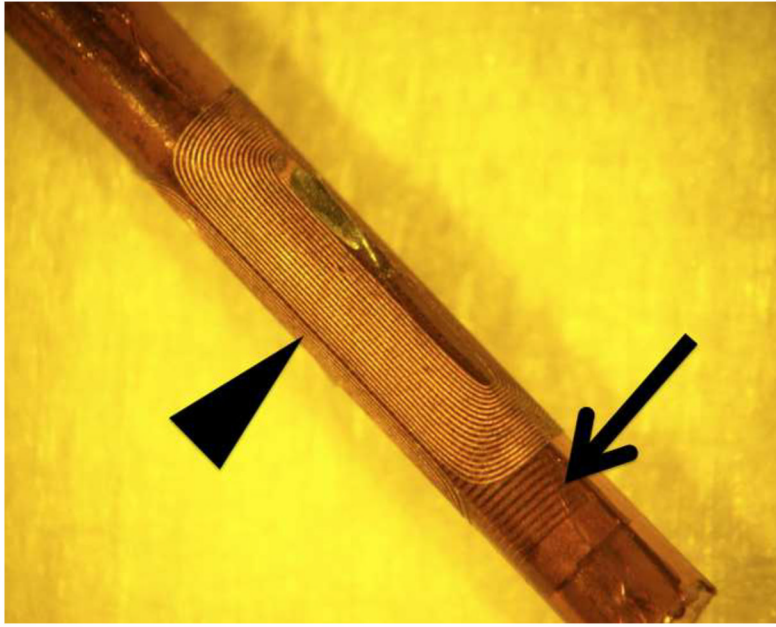


Figure 3. A 2-axis coil system demonstrating insertion of the helical coil (arrow) within the hollow polyimide tube mounted with the saddle coil (arrowhead).

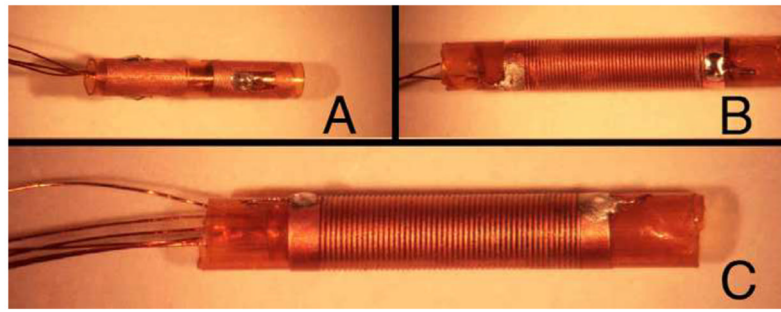


Figure 4. A 3-axis coil system

Panel A: A 2-axis orthogonal side-by-side saddle coils electrically connected to copper wire.

Panel B: A single axis helical coil electrically connected to copper wire.

Panel C: The 2-axis system has been placed in the 1-axis tube, forming a 3-axis system in which each axis will have a magnetic moment orthogonal to the other two.

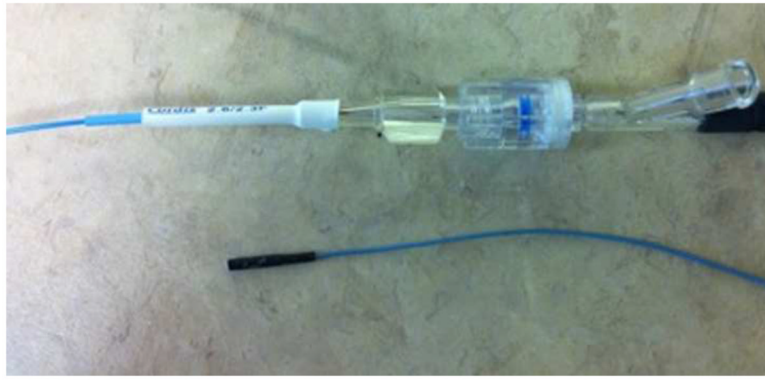


Figure 5. Coils shrink-wrapped on the tip of a microcatheter substrate. The final outer diameter of the catheter tip is approximately 2 mm (6 Fr).

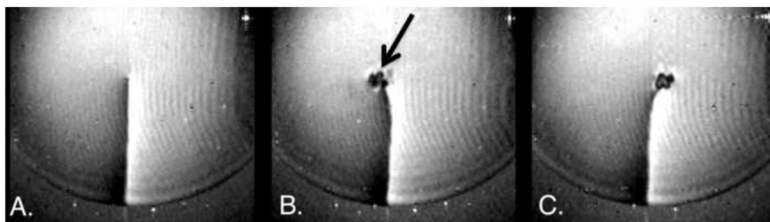


Figure 6. A microcatheter with a saddle coil mounted on the tip. The catheter coil construct is immersed in a water bath phantom, with b-FFE MR imaging at 1.5 T performed in the coronal plane

A. The catheter is clearly visible in the phantom prior to application of current to the coil.

B. Energizing the coil with +200 mA results in catheter tip deflection to the left, relative to the resting state. The magnetic field line artifact enhances visualization of the catheter tip (arrow).

C. Energizing the inner coil to -200 mA results in catheter tip deflection to the right.

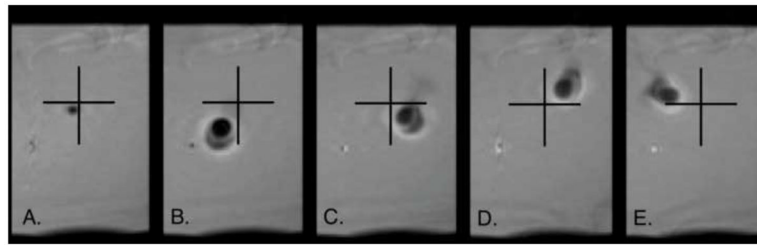


Figure 7. A 2-axis coil system in a water bath phantom, with b-FFE images obtained in the axial plane. The inner coil is helical while the outer coil is saddle in configuration (as shown in Fig. 5)

A. The tips of the non-energized coils are visualized in the phantom.

B. Energizing the inner coil to +100 mA and the outer coil to +100 mA results in movement to the left lower quadrant relative to the resting state.

C. Energizing the inner coil to -100 mA and the outer coil to +100 mA results in movement to the right lower quadrant.

D. Energizing the inner coil to -100 mA and the outer coil to -100 mA results in movement to the right upper quadrant.

E. Energizing the inner coil to +100 mA and the outer coil to -100 mA results in movement to the left upper quadrant.

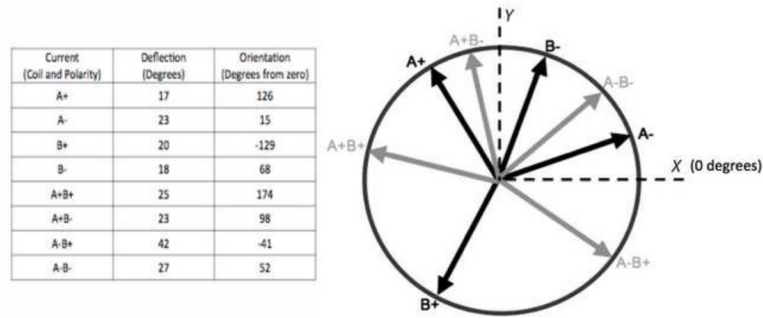


Figure 8. Summary of the 2-axis coil experiments. The table lists the longitudinal plane angle of deflection and the relative orientation of the catheter tip as a result of currents applied to the orthogonal coils with varying amplitudes and polarities. The associated pinwheel diagram graphically shows the orientation of the catheter tip in the axial plane, relative to the x-axis (0 degrees).

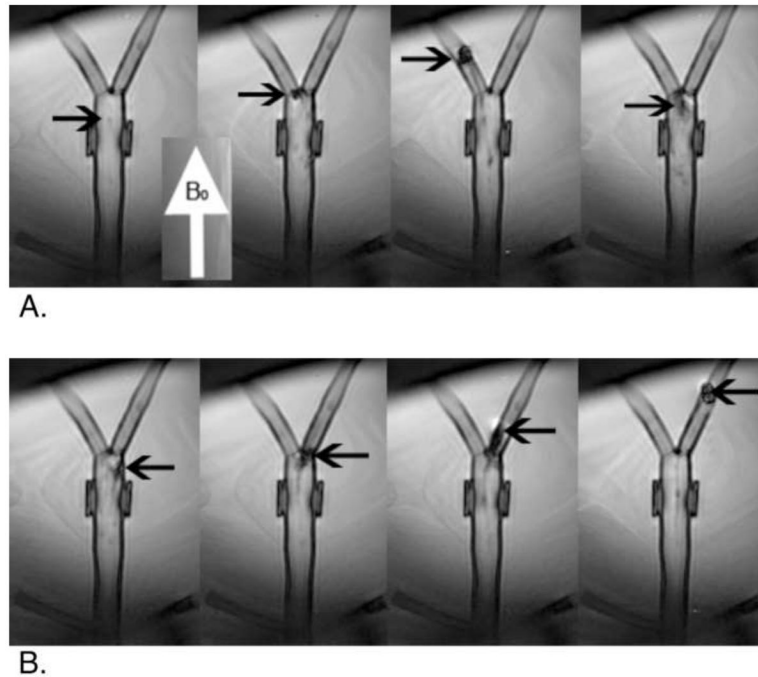


Figure 9. Sequential b-FFE MR images of a saddle-coil catheter in a bifurcated water-filled phantom

A. Positive current applied to the coil allows for deflection and movement of the catheter tip (arrow) into the left limb of the phantom.

B. Negative current applied to the coil allows for deflection and movement of the catheter tip (arrow) into the right limb of the phantom.

Table 1

Water Bath Phantom Deflections (2 cm Unrestrained Length)

Current	Deflection Angle (°)(Investigator #1)	Deflection Angle (°)(Investigator #2)	Mean Deflection Angle ± Standard Deviation (°)
0	0	0	0
100	26.5	25	25.75 ± 1.06
190	36.9	30	33.45 ± 4.87
350	56.3	45	50.65 ± 7.99

Table 2

Water Bath Phantom Deflections (5 cm Unrestrained Length)

Current	Deflection Angle (°)(Investigator #1)	Deflection Angle (°)(Investigator #2)	Mean Deflection Angle ± Standard Deviation (°)
0	0	0	0
50	14.6	15	14.8 ± 0.28
100	19.8	20	19.9 ± 0.14
190	27.5	30	28.75 ± 1.76
350	44.4	45	44.7 ± 0.42